ECA-BLS: An Efficient Complex-Augmented Broad Learning System

A. Rahaman
Department of Mathematics
Indian Institute of Technology Indore
Indore, India
phd2401141001@iiti.ac.in

A. Quadir
Department of Mathematics
Indian Institute of Technology Indore
Indore, India
mscphd2207141002@iiti.ac.in

M. Sajid
Department of Mathematics
Indian Institute of Technology Indore
Indore, India
phd2101241003@iiti.ac.in

M. Akhtar
Department of Mathematics
Indian Institute of Technology Indore
Indore, India
phd2101241004@iiti.ac.in

M. Tanveer
Department of Mathematics
Indian Institute of Technology Indore
Indore, India
mtanveer@iiti.ac.in

***Abstract*—Broad Learning System (BLS) is an efficient alternative to deep architectures due to its fast training, analytical learning, and strong generalization under limited data. However, existing BLS variants are confined to real-valued representations, restricting their ability to capture nonlinear interactions and second-order statistical dependencies inherent in real-world data. Notably, no prior BLS model fully exploits the complete second-order statistics that naturally emerge when data are embedded in the complex domain. To address this limitation, this paper introduces the first complex augmented Broad Learning System (CA-BLS), which transforms real-valued inputs into phase-encoded complex representations and adopts widely linear modeling to jointly leverage covariance and pseudo-covariance information via complex conjugate augmentation. This enables effective modeling of latent nonlinearities, coherence structures, and second-order dependencies inaccessible to conventional BLS formulations. To mitigate the additional computational cost of complex augmentation, an Efficient Complex Augmented BLS (ECA-BLS) is further developed, reformulating CA-BLS entirely in the real domain while preserving its exact decision function, achieving up to 75% fewer multiplications and over 60% fewer additions. A rigorous theoretical analysis proves the mathematical equivalence between CA-BLS and ECA-BLS, ensuring zero theoretical loss. Extensive experiments on 26 benchmark datasets from the UCI and KEEL repositories demonstrate that ECA-BLS consistently outperforms classical BLS and recent state-of-the-art randomized neural networks in accuracy, average rank, and statistical significance, establishing augmented second-order modeling as a critical and previously missing dimension of BLS research. The supplementary material is available in an anonymous repository at https://github.com/AnonymousAuthor0011/ECA-BLS.**

***Index Terms*—Randomized neural networks, Broad learning system, Complex Augmented, Second-order statistics.**

I. Introduction and Motivation

IN today's world, deep learning has become an inevitable research focus in the field of artificial intelligence to handle complex tasks such as image classification [1] and natural language processing [2], etc. Although deep learning has powerful learning capabilities, its complicated architecture and a vast number of hyperparameters make the training process extremely time-consuming and require powerful hardware to run the deep model. Therefore, consering these above issues, Chen and Liu proposed a broad learning system (BLS) [3]. BLS belongs to the family of randomized neural networks (RdNNs) [4] as RdNNs incorporate randomness in the topology and learning process of the model, resulting in RdNNs learning with fewer tunable parameters in less time and hardware resources. Thus, BLS has the advantages of a simple architecture and can learn with first speed. BLS has three primary layers: (i) a feature learning layer, (ii) an enhancement layer, and (iii) an output layer. In feature learning and enhancement layers. In the feature learning and enhancement segment, the input data are transformed into a high-dimensional feature space using a set of random projection mappings. As a result of the feature learning and enhancement segment, a collection of high-dimensional features is produced that effectively extracts important information from the input data. To train the BLS model, only the output layer parameters need to be computed by the least-squares method, resulting in no need for backpropagation during training. Further, the BLS has more advantages, like its ability to learn from a small number of training samples without overfitting, the universal approximation capability of BLS [3] makes it more promising among researchers, and the adaptable topology of BLS makes it possible to train and update the model effectively in an incremental way [3], and when training data are scarce, BLS may have superior generalization performance than deep learning models [5].

In recent years, a wide range of BLS variants have been proposed to enhance learning efficiency, robustness, and generalization across diverse application domains [6]. These efforts have significantly enriched the BLS framework while also revealing its inherent limitations [7]. For instance, an iterative gradient-descent-based learning strategy was introduced in [8] to update the connections among feature nodes, enhancement nodes, and output nodes, thereby improving adaptability beyond the original closed-form solution. To incorporate human-like reasoning into BLS, Shuang et al. [9] proposed a fuzzy BLS that integrates IF–THEN fuzzy rules with the BLS learning architecture. Subsequently, fuzzy BLS (F-BLS) and intuitionistic fuzzy BLS (IF-BLS) models were developed in [10] to enhance robustness against noise and outliers by explicitly modeling uncertainty and hesitation in training samples.

Further, the graph-embedding intuitionistic fuzzy adaptive BLS (GEIB) [11] was introduced to address imbalanced and noisy data by preserving the intrinsic geometric structure of the data manifold. This was achieved by embedding graph-based relations into the BLS framework and assigning adaptive importance scores to training samples using affiliation and non-affiliation degrees from intuitionistic fuzzy theory. More recently, the kernel risk-sensitive mean p-power BLS (KRPBLS) [12] was proposed to mitigate the sensitivity of conventional BLS models to label noise by replacing the minimum mean square error criterion with a more robust risk-sensitive optimization objective. Collectively, these studies have substantially improved the flexibility and resilience of BLS models, establishing them as competitive shallow learning architectures in modern machine learning.

Despite these advances, a fundamental limitation remains largely unaddressed. The performance of BLS is highly dependent on the feature learning and enhancement layers, which play a pivotal role in propagating information to the output layer. In standard BLS architectures, hidden-layer representations are generated through random projections. While computationally efficient, this random generation mechanism often fails to adequately capture complex nonlinear structures and higher-order dependencies inherent in real-world data, thereby restricting the representational capacity of the model.

In parallel, complex-valued neural networks (CVNNs) have attracted increasing attention due to their superior ability to model nonlinear relationships and signal coherence [13]. Unlike real-valued neural networks (RVNNs), CVNNs offer a natural and mathematically elegant framework for representing physical systems and signals encountered in many engineering applications. Notably, Hirose demonstrated that CVNNs often exhibit smaller generalization errors than their real-valued counterparts, owing to their enhanced capability to capture phase and amplitude interactions [14]. Zhang further showed that complex-valued gradient learning with complex step sizes provides theoretical and practical advantages over traditional real-valued learning [15]. More recently, a complex variant of a shallow RdNN was proposed in [16], where real-valued tabular data are transformed into complex representations and processed using complex weights and activation functions.

Importantly, recent advances in complex statistics indicate that the second-order characteristics of complex-valued data cannot be fully described by the conventional covariance matrix alone. Instead, both the covariance and pseudo-covariance matrices are required to capture the complete second-order statistics [17]. To address this issue, complex augmented valued neural networks based on widely linear modeling have been proposed [18], where the complex signal and its conjugate are jointly processed to exploit all available statistical information.

However, despite the strong theoretical foundations and empirical success of augmented CVNNs, their application has been largely confined to domains where data are inherently complex-valued, such as signal processing and communications. To the best of our knowledge, no complex augmented -valued variant of the Broad Learning System has been developed so far. Consequently, existing BLS models are unable to exploit signal coherence, full second-order statistics, and conjugate information, leaving a significant representational gap, particularly when dealing with nonlinear, noisy, or structurally complex tabular data.

Motivated by this clear gap, this paper proposes a novel Complex Augmented Broad Learning System (CA-BLS) that integrates complex augmented representations into both the feature learning and enhancement layers. By incorporating the complex conjugates of these layers, the proposed model is able to capture the complete second-order statistics of the data, including both covariance and pseudo-covariance components, thereby uncovering nonlinear structures that remain inaccessible to real-valued BLS models. While this augmentation significantly enhances representational power, it also introduces additional computational overhead due to the increased dimensionality of complex-valued matrices involved in pseudo-inverse computation.

To address this challenge, we further propose an Efficient Complex Augmented BLS (ECA-BLS), which substantially reduces computational complexity by replacing most complex-valued matrix operations with equivalent real-valued computations, without compromising model performance. Moreover, we rigorously prove the mathematical equivalence between CA-BLS and ECA-BLS, ensuring that the efficiency gains are achieved without any loss of modeling capability.

The primary contributions of this paper can be summarized as follows:

- A novel mechanism is introduced to transform real-valued tabular datasets into complex-valued representations.
- A Complex Augmented Broad Learning System (CA-BLS) is developed, employing complex weights and analytic activation functions to capture full second-order statistics.
- An Efficient Complex Augmented BLS (ECA-BLS) is proposed to significantly reduce the computational complexity of CA-BLS.
- A theoretical proof is provided to establish the equivalence between CA-BLS and ECA-BLS.
- Comprehensive experimental evaluations demonstrate the superiority of ECA-BLS over recent state-of-the-art models across diverse benchmark datasets.

Related works are given in Section S.I. of the Supplementary Material.

II. NOTATION

Let the training dataset be denoted as $\mathcal{Z}_{\text{raw}} = \{(x_j, y_j) \mid x_j \in \mathbb{R}^B,\, y_j \in \mathbb{R}^C,\, j = 1, 2, \ldots, D\}$, where B represents the number of features, C denotes the number of output classes, and D is the total number of training samples. The input samples are arranged into a data matrix $\mathbf{Z} \in \mathbb{R}^{D\times B}$, while the corresponding target labels are collected into a matrix $\mathbf{X} \in \mathbb{R}^{D\times C}$.

III. Proposed method

A. Transformation of Data from Real Field to Complex Field

To enable BLS to operate in the complex domain, each real-valued input feature is independently transformed into a complex-valued representation using phase encoding. Given a $(i,j)^{th}$ normalized real-valued input feature of real valued feature matrix $\mathbf{Z}$, $z_{ij} \in [0,1]$, its complex-valued representation is defined as

$$^{cx}z_{ij} = e^{(i\pi z_{ij})}, \tag{1}$$

where $i = \sqrt{-1}$, $i = 1, 2, \ldots, D$, and $j = 1, 2, \ldots, B$. This transformation maps real-valued features onto the unit circle in the complex plane, ensuring bounded magnitude and numerical stability. Moreover, phase encoding introduces nonlinear angular separation between samples, thereby enhancing class discriminability without increasing the dimensionality of the input space. After transformation, the real-valued dataset $\mathbf{Z} \in \mathbb{R}^{D\times B}$ is converted into a complex-valued dataset $^{cx}\mathbf{Z} \in \mathbb{C}^{D\times B}$, which serves as the input to the proposed complex-valued BLS framework.

B. Proposed Complex Augmented Broad Learning System (CA-BLS)

Although complex-valued data representations can effectively exploit phase information and enhance nonlinear modeling capability, they are still insufficient to fully characterize the second-order statistics of complex-valued signals when only covariance information is considered [17]. According to the theory of complex-valued random processes, the covariance matrix alone cannot completely describe non-circular complex signals. In such cases, the pseudo-covariance matrix carries additional and essential statistical information.

Phase-encoded complex representations derived from real-valued data are generally non-circular. Consequently, ignoring pseudo-covariance information may lead to suboptimal learning performance. To overcome this limitation, we adopt the principle of complex augmented modeling and propose an *Complex Augmented Broad Learning System (CA-BLS)*, which explicitly incorporates conjugate representations to fully exploit complete second-order statistics, thereby improving generalization capability.

Let $^{cx}\mathbf{Z} \in \mathbb{C}^{D\times B}$ denote the phase-encoded complex-valued input matrix, and let $\mathbf{X} \in \mathbb{R}^{D\times C}$ represent the corresponding target label matrix. Following the standard BLS architecture, the complex-valued input is mapped to the feature and enhancement layers using randomly generated complex weights, as described below.

1) Feature Learning Segment: Assume that the feature learning layer consists of a feature groups, each containing b nodes. The output of the ith feature group is defined as

$$^{cx}\mathbf{A}_i = {}^{cx}\sigma_i\big({}^{cx}\mathbf{Z}\,{}^{cx}\mathbf{W}_{A_i} + {}^{cx}\boldsymbol{\xi}_{A_i}\big) \in \mathbb{C}^{D\times b}, \quad i = 1, 2, \ldots, a, \tag{2}$$

where $^{cx}\sigma_i(\cdot)$ denotes the complex-valued activation function, $^{cx}\mathbf{W}_{A_i} \in \mathbb{C}^{B\times b}$ is a randomly generated weight matrix, and $^{cx}\boldsymbol{\xi}_{A_i} \in \mathbb{C}^{D\times b}$ is the corresponding bias matrix. The outputs of all feature groups are concatenated to form

$$^{cx}\mathbf{A}^a = \big[{}^{cx}\mathbf{A}_1, {}^{cx}\mathbf{A}_2, \ldots, {}^{cx}\mathbf{A}_a\big] \in \mathbb{C}^{D\times ab}. \tag{3}$$

2) Enhancement Segment: The augmented feature matrix $^{cx}\mathbf{A}^a$ is further projected into the enhancement layer through random complex transformations followed by nonlinear activation. Let c denote the number of enhancement groups, each consisting of d nodes. The output of the kth enhancement group is given by

$$^{cx}\mathbf{Y}_k = {}^{cx}\zeta_k({}^{cx}\mathbf{A}^a\,{}^{cx}\mathbf{W}_{Y_k} + {}^{cx}\boldsymbol{\Gamma}_{Y_k}) \in \mathbb{C}^{D\times d}, \quad k = 1, 2, \ldots, c, \tag{4}$$

where $^{cx}\zeta_k(\cdot)$ denotes the complex-valued activation function, $^{cx}\mathbf{W}_{Y_k} \in \mathbb{C}^{ab\times d}$ is a randomly generated weight matrix, and $^{cx}\boldsymbol{\Gamma}_{Y_k} \in \mathbb{C}^{D\times d}$ is the corresponding bias matrix. The enhancement outputs are concatenated as

$$^{cx}\mathbf{Y}^c = \big[{}^{cx}\mathbf{Y}_1, {}^{cx}\mathbf{Y}_2, \ldots, {}^{cx}\mathbf{Y}_c\big] \in \mathbb{C}^{D\times cd}. \tag{5}$$

3) Output Segment and Augmented Modeling: The feature and enhancement matrices are concatenated to form the complex hidden-layer output matrix

$$\mathbf{H} = \big[{}^{cx}\mathbf{A}^a, {}^{cx}\mathbf{Y}^c\big] \in \mathbb{C}^{D\times(ab+cd)}. \tag{6}$$

To capture the complete second-order statistics, including both covariance and pseudo-covariance information, we construct the augmented hidden matrix as

$$\mathbf{H}_a = [\mathbf{H}, \mathbf{H}^*] \in \mathbb{C}^{D\times 2(ab+cd)}, \tag{7}$$

where $(\cdot)^*$ denotes complex conjugation. The output weights of CA-BLS are obtained by solving the regularized least-squares problem

$$\arg\min_{\boldsymbol{\beta}_a} \frac{1}{2}\|\mathbf{H}_a\boldsymbol{\beta}_a - \mathbf{X}\|_2^2 + \frac{\lambda_a}{2}\|\boldsymbol{\beta}_a\|_2^2, \tag{8}$$

where $\boldsymbol{\beta}_a \in \mathbb{C}^{2(ab+cd)\times C}$ denotes the output weight matrix and λ_a is a regularization parameter. The closed-form solution is given by

$$\boldsymbol{\beta}_a = (\mathbf{H}_a^H\mathbf{H}_a + \lambda_a\mathbf{I})^{-1}\mathbf{H}_a^H\mathbf{X}, \tag{9}$$

where $(\cdot)^H$ denotes the Hermitian transpose and $\mathbf{I}$ is an identity matrix of appropriate dimension.

C. Efficient Complex Augmented Broad Learning System (ECA-BLS)

Although CA-BLS significantly enhances modeling capability by exploiting complete second-order statistics, the augmentation process doubles the number of hidden nodes and

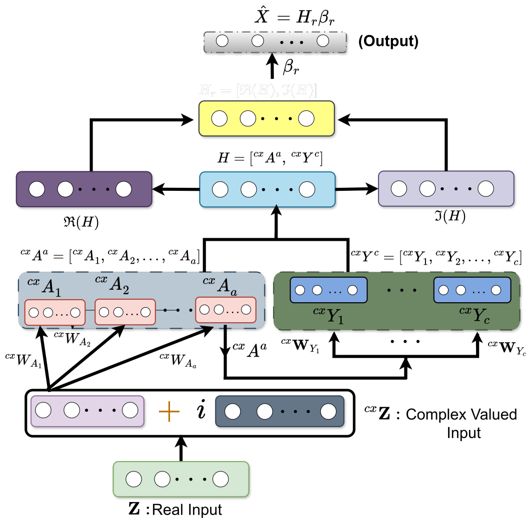

Fig. 1: Architecture of ECA-BLS.

requires complex-valued matrix inversion, leading to increased computational cost. To address this issue, we propose a computationally efficient reformulation termed as *Efficient Complex Augmented Broad Learning System (ECA-BLS)*. Figure 1 illustrates the architecture of ECA-BLS. The real-valued input is first transformed into the complex domain using phase encoding. Complex-valued feature and enhancement representations are then constructed following the BLS framework. Instead of explicitly forming the complex augmented matrix, ECA-BLS employs a real-valued augmentation strategy to implicitly capture conjugate information while significantly reducing computational complexity. Given the matrix $\mathbf{H}$ in (6), its real-valued augmented representation is defined as

$$\mathbf{H}_r = [\Re(\mathbf{H}), \Im(\mathbf{H})] \in \mathbb{R}^{D \times 2(ab+cd)}, \tag{10}$$

where $\Re(\cdot)$ and $\Im(\cdot)$ denote the real and imaginary parts, respectively. The output weights of ECA-BLS are obtained by solving

$$\arg\min_{\boldsymbol{\beta}_r} \frac{1}{2}\|\mathbf{H}_r\boldsymbol{\beta}_r - \mathbf{X}\|_2^2 + \frac{\lambda_r}{2}\|\boldsymbol{\beta}_r\|_2^2, \tag{11}$$

where $\boldsymbol{\beta}_r \in \mathbb{R}^{2(ab+cd)\times C}$ and λ_r is a regularization parameter. The closed-form solution is

$$\boldsymbol{\beta}_r = (\mathbf{H}_r^T\mathbf{H}_r + \lambda_r\mathbf{I})^{-1}\mathbf{H}_r^T\mathbf{X}. \tag{12}$$

Algorithm and complexity of the proposed ECA-BLS are given in given in Section S.III. and S.IV. of Supplementary Material, respectively.

D. Theoretical Justification of Equivalence between Proposed CA-BLS and ECA-BLS

The theoretical proof of equivalence between Proposed CA-BLS and ECA-BLS is given in Section S.II. of Supplementary Material.

The theoretical proof establishes a fundamental duality between the complex and real formulations:

- Mathematical Isomorphism: CA-BLS and ECA-BLS are algebraically isomorphic. The transformation matrix $\mathbf{V}$ defines a bijective mapping between the complex augmented feature space and the real expanded feature space, proving that both models optimize the exact same objective function in different coordinate systems.
- Preservation of Phase Information: ECA-BLS is not a simplification that discards complex characteristics. Instead, it implicitly captures the full phase-amplitude relationships of the widely linear model by encoding them within the cross-correlations of the separated real and imaginary channels.
- Zero Theoretical Loss: The proof guarantees that the output equivalence is exact, not approximate. Provided the regularization scaling $\lambda_a = 2\lambda_r$ is maintained, the real-valued implementation achieves the identical decision boundary as the complex-valued formulation with zero loss in accuracy.
- Computational Efficiency: While theoretically equivalent, ECA-BLS is computationally superior. By avoiding complex arithmetic where a single multiplication requires four real multiplications and two additions, ECA-BLS leverages highly optimized standard real-valued linear algebra, significantly reducing computational cost and memory overhead.

Based on this theoretical equivalence between CA-BLS and ECA-BLS, and the efficiency of ECA-BLS, we have conducted the experiments in the ECA-BLS to compare the performance and statistical significance of our proposed models.

S.V. Experimental Setup, Compared Models and Datasets

Detailed experimental setup, compared models, and datasets are discussed in Section S.V. in Supplementary Material.

E. Evaluation on UCI and KEEL Dataset

Table I summarizes the experimental results obtained on 26 benchmark datasets from the KEEL and UCI repositories, reporting classification accuracy for each method along with the corresponding average accuracy and average rank. The complete set of results, including the optimal hyperparameter configurations for the proposed model across all datasets, is provided in the Supplementary Material (Table II). Across all evaluated datasets and competing methods, the proposed ECA-BLS consistently demonstrates superior performance. In particular, ECA-BLS achieves the highest average classification accuracy of 84.5337%, clearly outperforming all baseline and state-of-the-art models considered in this study. The closest competitors, KRPBLS and GEIB, attain average accuracies of 80.9% and 80.7861%, respectively, resulting in a substantial performance margin in favor of ECA-BLS. All remaining state-of-the-art methods achieve average accuracies below 80%, further emphasizing the effectiveness of the proposed approach.

TABLE I: Classification accuracies along with average accuracy and average rank for ECA-BLS model evaluated against baseline models on 26 UCI and KEEL datasets.

Dataset ↓ | Model →	BLS[3]	H-ELM[19]	GEIB [11]	F-BLS [10]	IF-BLS [10]	KRP-BLS [12]	**ECA-BLS**†
acute_inflammation	88.8889	91.6667	100	86.1111	100	100	100
bank	88.5041	88.8643	71.4602	85.409	89.1673	88.1356	88.1356
brwisconsin	92.1951	87.2549	96.5686	89.7561	63.4146	92.6829	87.8049
chess_krvkp	91.9708	80.65	84.9687	85.09	86.1314	85.4015	93.8478
cleve	82.2222	75.2809	83.1461	56.6667	82.2222	80	85.5556
ecoli-0-1_vs_5	94.4444	88.89	97.2222	90.94	51.3889	62.5	88.8889
ecoli-0-1-4-7_vs_2-3-5-6	90.099	87.13	75	90.1	90.099	90.099	88.1188
ecoli-0-1-4-7_vs_5-6	93	93	74.7475	94	91	95	90
ecoli-0-6-7_vs_5	60.6061	90.9091	90.9091	66.6667	98.4848	93.9394	90.9091
haber	78.2609	82.61	70.3297	76.26	79.3478	78.2609	79.3478
heart_hungarian	80.8989	64.7727	80.6818	59.5506	79.7753	74.1573	80.8989
heart-stat	87.6543	80.21	81.4815	78.89	85.1852	88.8889	82.716
ionosphere	86.7925	78.0952	88.5714	81.1321	86.7925	85.8491	83.0189
led7digit-0-2-4-5-6-7-8-9_vs_1	73.6842	80.23	91.6667	80.45	47.3684	75.188	90.9774
mammographic	79.5848	78.94	80.9028	78.89	82.0069	79.2388	83.045
monk1	41.3174	46.988	37.3494	49.1018	46.1078	55.0898	54.491
musk_1	76.9231	75.15	69.0141	78.32	79.7203	80.4196	90.2098
oocytes_merluccius_nucleus_4d	56.6775	70.18	72.549	72.2	75.57	74.9186	73.6156
ozone	85.5834	96.58	83.6842	96.58	80.1564	83.1731	96.5834
ripley	89.3333	60.8	92	84.2667	88.8	88.5333	70.1333
shuttle-6_vs_2-3	94.2029	95.65	92.2754	100	100	92	97.1014
spambase	82.042	69.27	87.7536	65.89	82.5455	70.6731	86.097
spectf	81.4815	75.75	67.5	80.32	75.3086	77.7778	82.716
vertebral_column_2clases	65.5591	69.89	72.043	65.56	64.2308	64.4086	69.8925
wpbc	71.1864	77.97	75.1724	76.27	70.5932	59.322	77.9661
yeast-2_vs_4	83.871	82.81	83.4416	82.39	94.8387	87.7419	85.8065
Average Accuracy	80.6532	79.5978	80.7861	78.8773	79.6252	80.9	**84.5337**
Average rank	3.9423	**4.7692**	4.0577	4.6923	3.75	3.8654	**2.9231**

These results provide strong empirical evidence that the proposed ECA-BLS offers enhanced generalization capability and robustness across a wide range of data distributions. **Statistical rank:** Average accuracy may be biased by exceptional performance on individual datasets and does not always reflect a model's overall robustness. To obtain a fairer evaluation, we adopt a ranking-based assessment [20], where models are evaluated independently on each dataset. Lower ranks are assigned to better-performing models, while higher ranks indicate poorer performance. Given u models evaluated over v datasets, let R_r^s denote the rank of the r^{th} model on the s^{th} dataset. The average rank of the r^{th} model is computed as $R_r = \frac{1}{v}\sum_{s=1}^{v} R_r^s$, which provides an aggregated and unbiased measure of comparative performance across all datasets. The proposed ECA-BLS achieves the lowest average rank of 2.9231 among all compared methods, indicating the most consistent performance across the evaluated datasets. The second and third best positions are attained by IF-BLS and KRPBLS, respectively. In contrast, recent advanced baselines such as GEIB and F-BLS obtain noticeably higher average ranks of 4.0577 and 4.6923, respectively. Likewise, classical models, including H-ELM and BLS, exhibit inferior rankings of 4.7692 and 3.9423, further highlighting the competitive advantage of the proposed approach. Overall, the ranking-based analysis provides compelling statistical evidence that ECA-BLS delivers superior and more stable performance than both classical and state-of-the-art competitors, thereby confirming its strong generalization capability across diverse benchmark datasets.

Friedman test: The Friedman test [21] is employed to statistically examine whether significant performance differences exist among the compared models. Under the null hypothesis, all models are assumed to exhibit equivalent performance, corresponding to equal average ranks. The Friedman test statistic follows a chi-squared distribution, denoted by χ_F^2, with $(u-1)$ degrees of freedom, and is computed as$\chi_F^2 = \frac{12v}{u(u+1)}\left(\sum_{i=1}^{u} R_i^2 - \frac{u(u+1)^2}{4}\right)$, where u is the number of models, v is the number of datasets, and R_i denotes the average rank of the i^{th} model. To obtain a more accurate test under finite sample sizes, the Friedman statistic is further transformed into an F-statistic given by $F_F = \frac{(v-1)\chi_F^2}{v(u-1)-\chi_F^2}$, which follows an F-distribution with $(u-1)$ and $(v-1)(u-1)$ degrees of freedom. In our experiments, considering $u = 7$ models evaluated over $v = 26$ datasets, the computed statistics are $\chi_F^2 = 12.9142$ and $F_F = 2.2564$. At a significance level of 5%, the critical value of the F-distribution with $(6, 150)$ degrees of freedom is 2.1595. Since $F_F > 2.1595$, the null hypothesis is rejected, indicating statistically significant performance differences among the compared models. Sections S.VII., S.VIII., and S.IX of Supplementary Material discussed the Win–Tie–Loss (W–T–L) sign test, sensitivity analysis, and evaluation of the proposed ECA-BLS under contaminated Gaussian noise, respectively.

IV. Conclusion and Future Work

This paper fundamentally advances Broad Learning Systems by introducing complex augmented modeling into the BLS framework for the first time. Unlike existing BLS variants that focus on architectural or robustness enhancements within the real domain, the proposed approach overcomes the intrinsic inability of real-valued BLS to exploit complete second-order statistical information, thereby closing a long-standing gap in the literature. By employing phase-encoded complex and complex augmented representations within a widely linear learning formulation, the proposed CA-BLS jointly leverages covariance and pseudo-covariance information to capture nonlinear structures and coherence patterns that are inaccessible to conventional BLS models. To ensure computational efficiency and scalability, an equivalent real-domain formulation, termed ECA-BLS, is rigorously derived and proven to preserve the exact decision function of CA-BLS. Extensive experiments on diverse benchmark datasets, supported by Friedman and win–tie–loss statistical analyses, consistently demonstrate the superior generalization, robustness, and stability of ECA-BLS over classical BLS and recent state-of-the-art variants. Together, the theoretical guarantees and empirical evidence establish that complex augmented learning is a missing foundational component of BLS research. Consequently, this work elevates BLS from a purely real-domain randomized model to a more expressive, statistically complete, and practically deployable learning paradigm.

References

[1] Y. Sepehri, P. Pad, A. C. Yüzügüler, P. Frossard, and L. A. Dunbar, "Hierarchical training of deep neural networks using early exiting," *IEEE Transactions on Neural Networks and Learning Systems*, vol. 36, no. 4, pp. 6271–6285, 2024.

[2] E. De Santis, A. Martino, and A. Rizzi, "Human Versus Machine Intelligence: Assessing Natural Language Generation Models Through Complex Systems Theory," *IEEE Transactions on Pattern Analysis and Machine Intelligence*, vol. 46, no. 7, pp. 4812–4829, 2024.

[3] C. P. Chen and Z. Liu, "Broad learning system: An effective and efficient incremental learning system without the need for deep architecture," *IEEE transactions on neural networks and learning systems*, vol. 29, no. 1, pp. 10–24, 2017.

[4] L. Zhang and P. N. Suganthan, "A survey of randomized algorithms for training neural networks," *Information Sciences*, vol. 364, pp. 146–155, 2016.

[5] W. Yu and C. Zhao, "Broad convolutional neural network based industrial process fault diagnosis with incremental learning capability," *IEEE Transactions on Industrial Electronics*, vol. 67, no. 6, pp. 5081–5091, 2019.

[6] M. Tanveer, A. Mishra, M. Sajid, and A. Quadir, "BLS-CIL: Class Imbalance Broad Learning System via Dual Weighting and Layer Trimming," *Pattern Recognition*, vol. 174, p. 112940, 2026.

[7] M. Tanveer, M. Pathak, M. Sajid, A. Quadir, and Priyamvada, "Fuzzy-driven broad learning system with class probability and density awareness for multi-view data," *Neural Networks*, vol. 201, p. 108914, 2026.

[8] S. Feng and C. L. P. Chen, "Broad Learning System for Control of Nonlinear Dynamic Systems," in *2018 IEEE International Conference on Systems, Man, and Cybernetics (SMC)*, 2018, pp. 2230–2235.

[9] S. Feng and C. P. Chen, "Fuzzy broad learning system: A novel neuro-fuzzy model for regression and classification," *IEEE transactions on cybernetics*, vol. 50, no. 2, pp. 414–424, 2018.

[10] M. Sajid, A. K. Malik, and M. Tanveer, "Intuitionistic fuzzy broad learning system: Enhancing robustness against noise and outliers," *IEEE Transactions on Fuzzy Systems*, vol. 32, no. 8, pp. 4460–4469, 2024.

[11] W. Chen, K. Yang, Z. Yu, F. Nie, and C. L. P. Chen, "Adaptive Broad Network With Graph-Fuzzy Embedding for Imbalanced Noise Data," *IEEE Transactions on Fuzzy Systems*, vol. 33, no. 6, pp. 1949–1962, 2025.

[12] W. Deng, J. Shen, J. Ding, and H. Zhao, "Robust Dual-Model Collaborative Broad Learning System for Classification Under Label Noise Environments," *IEEE Internet of Things Journal*, vol. 12, no. 12, pp. 21 055–21 067, 2025.

[13] C. Lee, H. Hasegawa, and S. Gao, "Complex-Valued Neural Networks: A Comprehensive Survey," *IEEE/CAA Journal of Automatica Sinica*, vol. 9, no. 8, pp. 1406–1426, 2022.

[14] A. Hirose and S. Yoshida, "Generalization Characteristics of Complex-Valued Feedforward Neural Networks in Relation to Signal Coherence," *IEEE Transactions on Neural Networks and Learning Systems*, vol. 23, no. 4, pp. 541–551, 2012.

[15] H. Zhang and D. P. Mandic, "Is a Complex-Valued Stepsize Advantageous in Complex-Valued Gradient Learning Algorithms?" *IEEE Transactions on Neural Networks and Learning Systems*, vol. 27, no. 12, pp. 2730–2735, 2016.

[16] M. Sajid, M. Akhtar, A. Quadir, and M. Tanveer, "RVFL-X: A Novel Randomized Network Based on Complex Transformed Real-Valued Tabular Datasets," in *2025 International Joint Conference on Neural Networks (IJCNN)*. IEEE, 2025, pp. 1–8.

[17] Z. Qing, J. Ni, Z. Li, E. C. Mengüç, J. Chen, and D. P. Mandic, "Performance analysis of the augmented complex-valued least mean kurtosis algorithm," *Signal Processing*, vol. 203, p. 108792, 2023.

[18] D. Xu, H. Zhang, and D. P. Mandic, "Convergence analysis of an augmented algorithm for fully complex-valued neural networks," *Neural Networks*, vol. 69, pp. 44–50, 2015.

[19] J. Tang, C. Deng, and G.-B. Huang, "Extreme learning machine for multilayer perceptron," *IEEE transactions on neural networks and learning systems*, vol. 27, no. 4, pp. 809–821, 2015.

[20] J. Demšar, "Statistical comparisons of classifiers over multiple data sets," *The Journal of Machine Learning Research*, vol. 7, pp. 1–30, 2006.

[21] M. Friedman, "A comparison of alternative tests of significance for the problem of m rankings," *The Annals of Mathematical Statistics*, vol. 11, no. 1, pp. 86–92, 1940.